JACC: CASE REPORTS VOL. 3, NO. 7, 2021

CASE REPORT

ADVANCED

CLINICAL CASE

Extracardiac Accumulation of Technetium-99m-Pyrophosphate in Transthyretin Cardiac Amyloidosis

Koji Takahashi, MD,[a,b] Daisuke Sasaki, MRT,[c] Tomoki Sakaue, MD,[a,b] Daijiro Enomoto, MD,[b] Shigeki Uemura, MD,[b] Takafumi Okura, MD,[b] Shuntaro Ikeda, MD,[a,b] Daichi Yamamoto, MRT,[c] Taizo Kono, MRT,[c] Nobuhisa Yamamura, MLT[d]

ABSTRACT

This report presents a rare case of acute decompensated heart failure with technetium-99m-pyrophosphate accumulation in extracardiac sites, such as chest and abdominal walls, in addition to intense myocardial uptake of the tracer. Subsequently, an abdominal fat pad fine-needle aspiration biopsy, which provided positive findings for transthyretin amyloidosis, was performed. (**Level of Difficulty: Advanced.**) (J Am Coll Cardiol Case Rep 2021;3:1069–74) © 2021 The Authors. Published by Elsevier on behalf of the American College of Cardiology Foundation. This is an open access article under the CC BY-NC-ND license (http://creativecommons.org/licenses/by-nc-nd/4.0/).

HISTORY OF PRESENTATION

An 89-year-old Japanese woman was admitted to our hospital with a history of peripheral edema and dyspnea at rest; the oxygen saturation in room air was 80%, pulse rate 73 beats/min with an irregular rhythm, systemic blood pressure 116/73 mm Hg, and respiratory rate 14 breaths/min with oxygen saturation of 93% at a flow rate of 2 l/min over an oxygen mask. On auscultation, there was a third heart sound and a systolic regurgitant murmur; wet rales in the lung fields were audible. The liver was palpable by a 2-finger breadth below the costal margin. Marked pretibial edema and jugular venous distension were observed.

LEARNING OBJECTIVES

- To identify electrocardiogram and echocardiographic changes over time that are "red flags" for cardiac amyloidosis, which may occur at the timing of the subsequent ADHF in patients with chronic heart failure.
- To appropriately regulate the dosage of the antihypertensive and heart-failure drugs, such as calcium-channel blockers or renin-angiotensin-aldosterone system inhibitors, which are often poorly tolerated in cardiac amyloidosis.

PAST MEDICAL HISTORY

The patient's medical history included long-standing hypertension, and Alzheimer's disease resulting in a gradual cognitive decline; however, she had no history indicating a high index of suspicion for cardiac amyloidosis, such as carpal tunnel

From the [a]Department of Community Emergency Medicine, Ehime University Graduate School of Medicine, Ehime, Japan; [b]Department of Cardiology, Yawatahama City General Hospital, Ehime, Japan; [c]Department of Radiology, Yawatahama City General Hospital, Ehime, Japan; and the [d]Department of Clinical Pathology, Yawatahama City General Hospital, Ehime, Japan.
The authors attest they are in compliance with human studies committees and animal welfare regulations of the authors' institutions and Food and Drug Administration guidelines, including patient consent where appropriate. For more information, visit the Author Center.

Manuscript received September 16, 2020; revised manuscript received January 11, 2021, accepted February 17, 2021.

ISSN 2666-0849 https://doi.org/10.1016/j.jaccas.2021.02.015

ABBREVIATIONS AND ACRONYMS

ADHF = acute decompensated heart failure

ATTR-CM = transthyretin cardiac amyloidosis

CT = computed tomography

DPD = 3,3-diphosphono-1,2-propanedicarboxylic acid

HMDP = hydroxymethylene diphosphonate

LV = left ventricle

MR = mitral regurgitation

PYP = pyrophosphate

SPECT = single photon emission computed tomography

^{99m}Tc = technetium-99m

syndrome, lumbar spinal stenosis, biceps tendon rupture, or autonomic dysfunction.

Four years prior, she had been admitted due to acute decompensated heart failure (ADHF). An electrocardiogram revealed atrial fibrillation and complete right bundle branch block (Figure 1A). The echocardiogram demonstrated severe mitral regurgitation (MR) due to chordal rupture, a dilated left ventricle (LV) with end-diastolic dimension of 59.5 mm, dilated left atrium with volume of 88.1 ml/m^2, and normal interventricular septal wall thickness of 9.3 mm (Figure 2A). A mildly reduced LV ejection fraction of 46%, and slightly abnormal global LV longitudinal strain of −15.3% with apical-to-basal longitudinal strain ratio of 1.2 were observed. The patient had been diagnosed with ADHF due to severe MR resulting from chordal rupture, complicated by atrial fibrillation. Surgical repair of MR was not performed. She was discharged on 5 mg apixaban, 30 mg azosemide, 8 mg candesartan cilexetil, 25 mg spironolactone, and 2.5 mg amlodipine besylate daily.

DIFFERENTIAL DIAGNOSIS

The differential diagnosis included ADHF due to worsening MR or due to MR and another heart disease.

INVESTIGATIONS

Blood tests revealed a high-sensitivity cardiac troponin I level of 58.9 pg/mL and a brain natriuretic peptide level of 210.9 pg/mL, over the reference range (≤16.0 pg/mL and ≤18.4 pg/mL, respectively). The estimated glomerular filtration rate was 43 ml/min/1.73 m^2. A chest radiograph displayed cardiomegaly with pulmonary congestion and massive pleural effusion. An electrocardiogram revealed atrial fibrillation with low voltage, right axis deviation, and incomplete right bundle branch block (Figure 1B). The height in R-waves was decreased in all leads compared with that 4 years prior (Figure 1A). The echocardiogram demonstrated a dilated LV with end-diastolic dimension of 55.5 mm, dilated left atrium with volume of 95.5 ml/m^2, and an increase in the interventricular septum of 12.3 mm (Figure 2B). Mildly

FIGURE 1 Electrocardiograms Recorded Before and at Admission

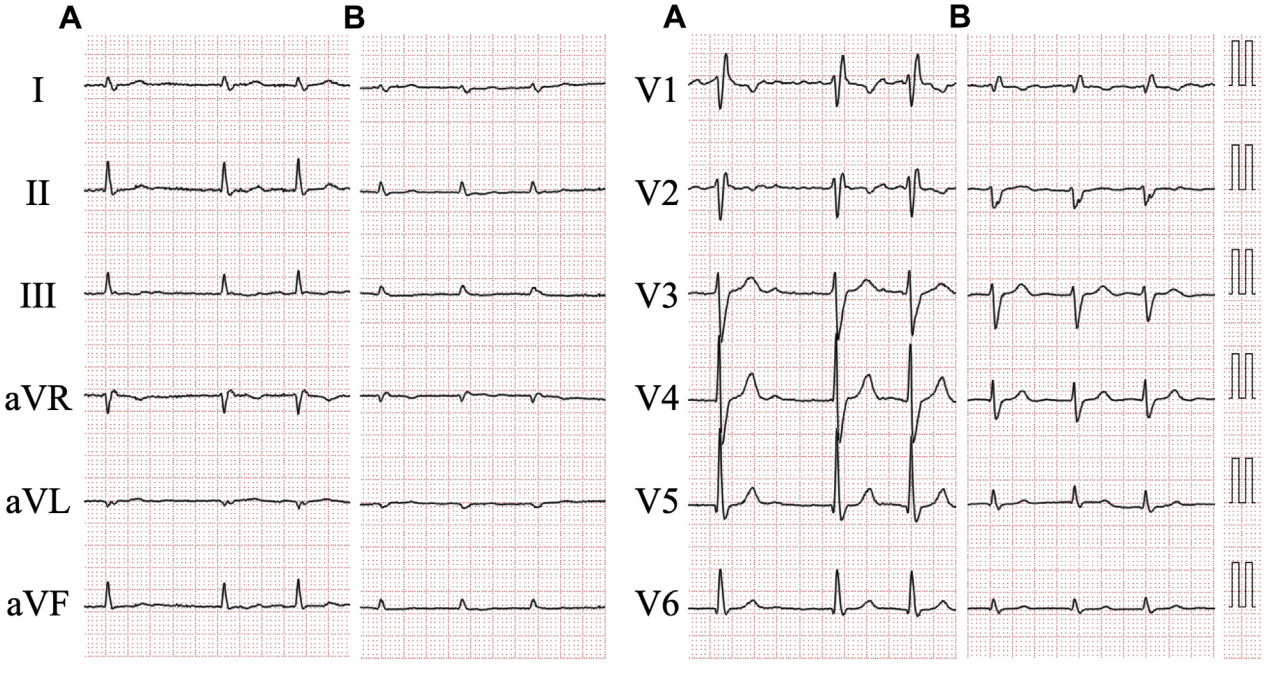

Electrocardiogram recorded 4 years before **(A)** and at admission **(B)**.

FIGURE 2 **Transthoracic Echocardiogram**

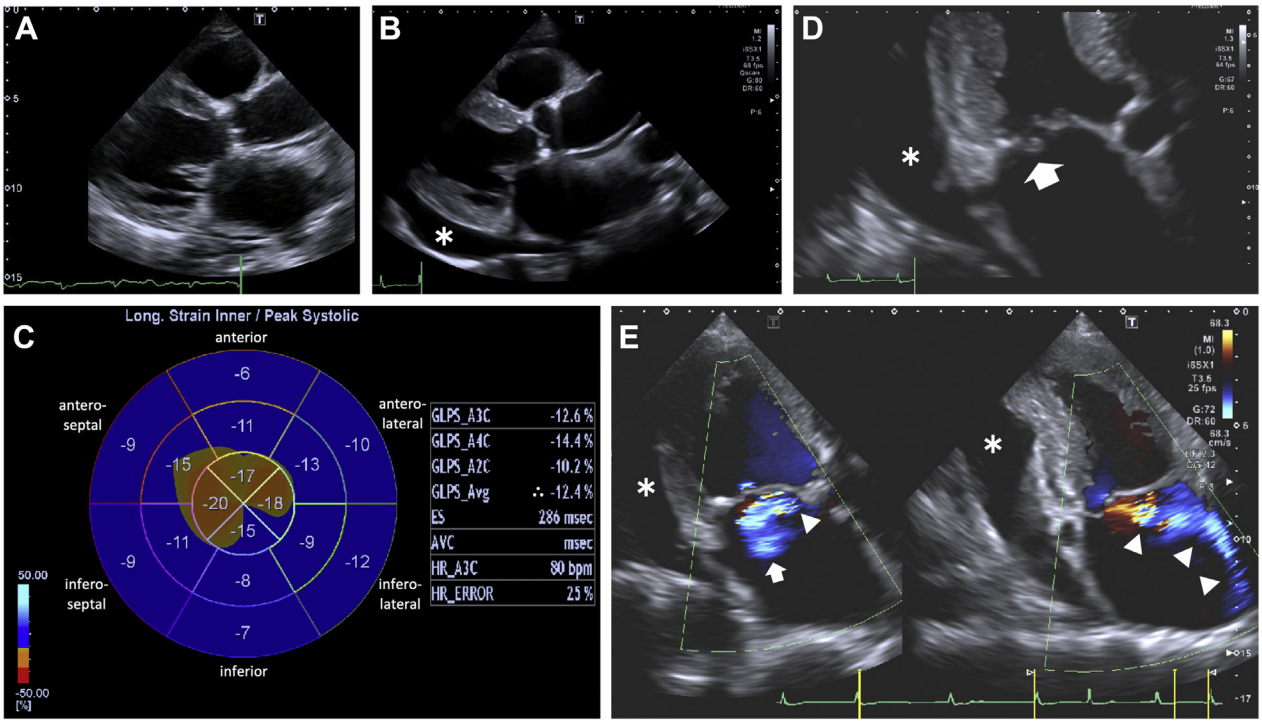

Echocardiograms recorded 4 years before **(A)** and at admission **(B to E)**. **(C)** The bull's eye map (with apex at the center of the color-coding map) illustrates segmental longitudinal left ventricular (LV) peak systolic strain values of 16-segment model, which were semiautomatically generated by speckle-tracking analysis of 2-dimensional LV images acquired from apical 2-, 3-, and 4-chamber views, and shows a reduced global longitudinal LV peak systolic strain value, calculated as the mean of these 16 values, of −12.4% (marked with an **asterisk**) with an apical-to-basal strain ratio, calculated as apical septal longitudinal strain divided by average basal septal (anteroseptal and inferoseptal) longitudinal strain, of 2.2 indicating apical sparing (>2.1). Two separate jets of mitral regurgitation (MR), of which one directed toward the center of the left atrium due to atrial functional MR **(small arrow)** and another directed eccentrically in connection with the aorta due to chordal rupture **(arrowheads),** are shown. **Asterisks and large arrows** indicate pericardial effusion and torn chordae of the mitral valve, respectively.

hypokinetic wall motions in the entire LV with an ejection fraction of 43% was accompanied by global LV longitudinal strain of −12.4% with apical-to-basal longitudinal strain ratio of 2.2 (Figure 2C). Ruptured chordae of the mitral valve with severe MR and pericardial effusion were also detected (Figures 2B, 2D, and 2E). The peak velocity across the tricuspid valve was 3.63 m/s, which is suggestive of pulmonary hypertension.

Because cardiac amyloidosis was suspected, technetium-99m (^{99m}Tc)-pyrophosphate (PYP) scintigraphy was performed. Chest-centered planar and single photon emission computed tomography (SPECT) images with fusion to computed tomography (CT) images were obtained 2 hours after intravenous injection of 20 mCi of the radiotracer. The acquisition protocol for both studies was as follows: end-expiratory breath-hold for CT imaging versus free-breathing for ^{99m}Tc-PYP SPECT imaging. A ^{99m}Tc-PYP scan showed grade 3 myocardial uptake with a heart/contralateral lung ratio of 1.6 (Figure 3). Marked accumulation of the tracer in the extracardiac sites, such as chest and abdominal walls, was observed (Figure 4). Due to this unexpected result in the ^{99m}Tc-PYP scan, SPECT images were obtained again 4 hours post intravenous injection of the radiotracer; most faded out, although some remained.

Serum and urine immunofixation tests revealed no immunoglobulin monoclonal proteins. However, serum free light chain kappa/lambda ratio of 2.01 was slightly elevated (reference range: 0.26 to 1.65). Subsequently, we performed an abdominal fat pad fine-needle aspiration biopsy with positive results for transthyretin amyloidosis. However, a gene sequencing test to establish wild-type transthyretin cardiac amyloidosis (ATTR-CM) versus variant-type ATTR-CM was not performed because the patient was unable to provide informed consent for the test.

FIGURE 3 ^{99m}Tc-PYP Scintigrams Showing Biventricular Myocardial Uptake of the Tracer

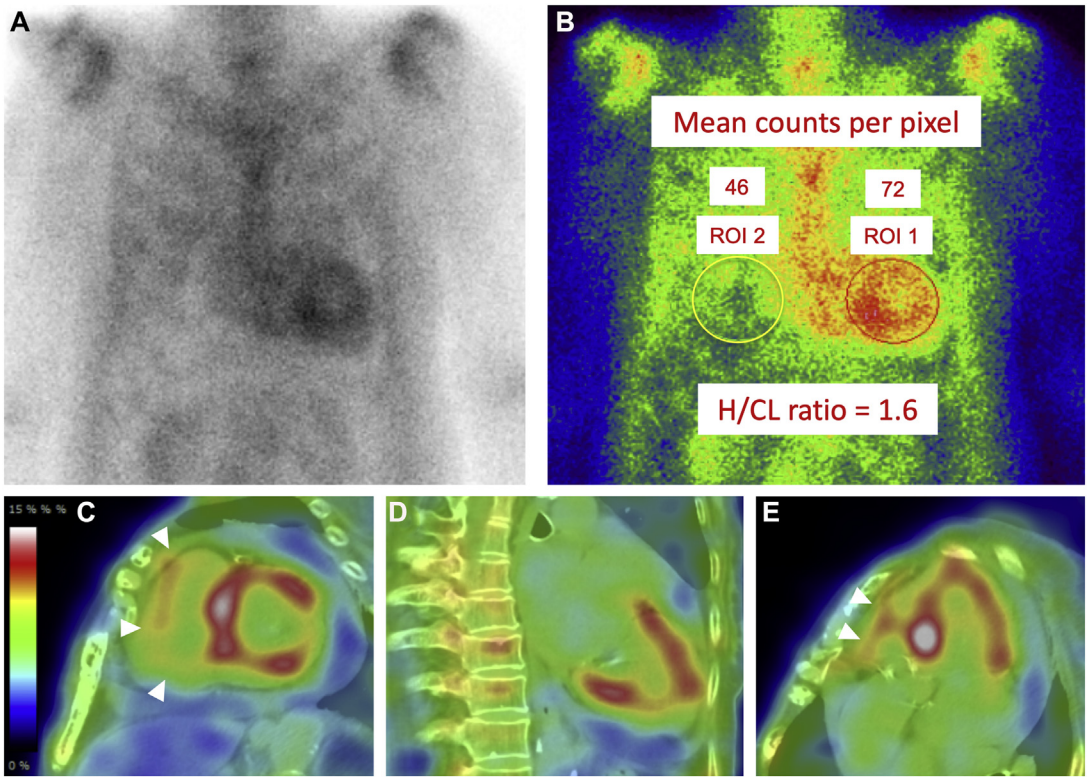

Technetium-99m-pyrophosphate (^{99m}Tc-PYP) planar imaging (anteroposterior view) **(A),** semi-quantitative heart-to-contralateral lung (H/CL) ratio on planar imaging **(B),** and single photon emission computed tomographic images with fusion to computed tomographic images—short-axis view **(C),** vertical long-axis view **(D),** horizontal long-axis view **(E)**—obtained 2 h after injection of the radiotracers. ROI 1 and ROI 2 indicate the regions of interest positioned to maximize the coverage of the heart without including the adjacent lung and to minimize the overlap with the sternal or focal rib uptake, respectively. **Arrowheads** indicate the uptake of ^{99m}Tc-PYP in the right ventricular myocardium.

MANAGEMENT

The patient was diagnosed with ADHF, of which the etiology was both ATTR-CM and severe MR mainly due to chordal rupture, complicated by atrial fibrillation. Daily intravenous injection of furosemide (40 mg) and oral tolvaptan (15 mg) did not show sufficient improvement. Thus, daily intravenous injection of potassium canrenoate (100 mg), followed by oral spironolactone (75 mg) were administered, leading to decreased congestion and symptomatic relief. Tafamidis meglumine was not administered because differentiation between the wild-type and the variant ATTR by genetic testing is a prerequisite for the drug to be prescribed in Japan.

DISCUSSION

Radionuclide imaging plays a critical role in the diagnosis and identification of ATTR-CM. Three tracers—^{99m}Tc-PYP, -3,3-diphosphono-1,2-propanedicarboxylic acid (DPD), and -hydroxymethylene diphosphonate (HMDP)—have been evaluated for imaging ATTR-CM, although these are not universally available (1,2). ^{99m}Tc-PYP is available in the United States, whereas ^{99m}Tc-DPD, and -HMDP are accessible in Europe. In Japan, ^{99m}Tc-PYP is most used. No direct comparison exists between these tracers. According to available information, they may be employed interchangeably. ^{99m}Tc-DPD/-HMDP, predominantly employed for whole body imaging,

FIGURE 4 **SPECT Images of ^{99m}Tc-PYP Scintigrams**

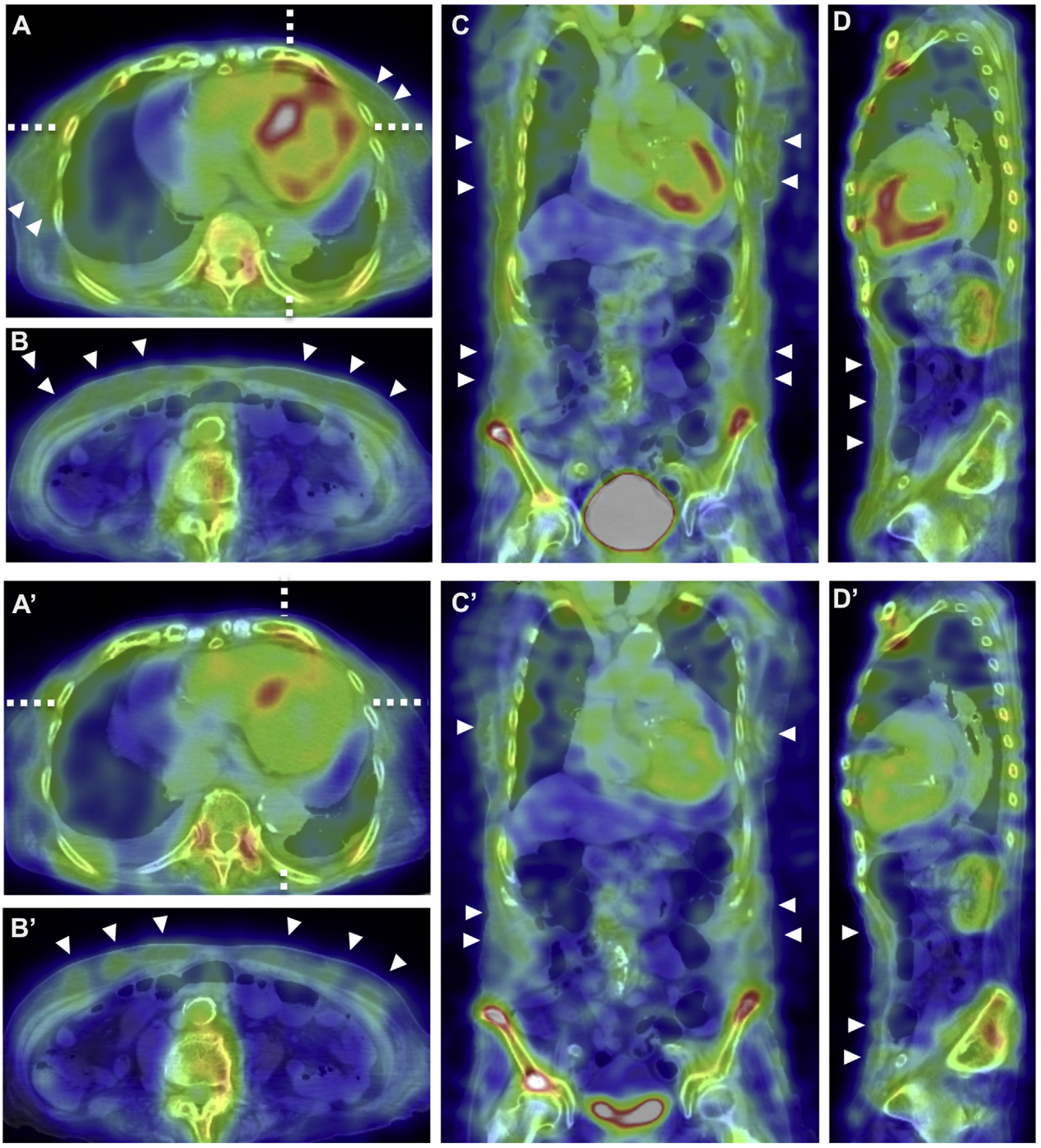

Single photon emission computed tomographic (SPECT) images of technetium-99m-pyrophosphate (^{99m}Tc-PYP) scintigrams with fusion to computed tomographic (CT) images obtained 2 h **(A to D)** and 4 h **(A′ to D′)** after injection of the radiotracers. Images show horizontal plane at the level of the heart and at the level of the umbilicus, respectively **(A/A′, B/B′)**; coronal plane **(C/C′)**; sagittal plane **(D/D′)**. Horizontal lines in **A/A′** indicate the level of the coronal slice shown by **C/C′**, and the vertical lines in **A/ A′** indicate the sagittal plane shown by **D/D′**, respectively. There is some misregistration of SPECT/CT fusion images resulting from patient movement and respiration. However, the impact on image interpretation due to this misregistration is minimal. **Arrowheads** indicate abnormal accumulation of ^{99m}Tc-PYP in chest and abdominal walls.

allows the detection of extracardiac amyloid infiltration. In contrast, whole body imaging for ^{99m}Tc-PYP does not provide additional diagnostic value (1). Reports regarding abnormal noncardiac accumulation of ^{99m}Tc-PYP, as clearly displayed in the patient, are limited (3). It is unclear why ^{99m}Tc-PYP markedly accumulated in extracardiac sites in the patient. However, this could indicate a large amyloid burden in the affected sites.

The precise diagnosis of ATTR-CM requires endomyocardial biopsy to demonstrate amyloid deposition. However, this procedure is relatively invasive and cannot be performed routinely. Sampling of an alternative tissue has minimized its need. For example, fine-needle aspiration of the abdominal fat pad is a safe screening procedure, although it has very low sensitivity because of small amyloid burden in ATTR-CM (4). In our patient, the unexpected result in the ^{99m}Tc-PYP scan guided the biopsy of the abdominal fat pad.

FOLLOW-UP

Hypotension occurred as water retention improved. Therefore, amlodipine besylate was terminated and the dosage of candesartan cilexetil was decreased from 8 mg to 4 mg daily. Our patient was not readmitted for ADHF over a 3-month follow-up.

CONCLUSIONS

In a patient with ATTR-CM, ^{99m}Tc-PYP imaging demonstrated extracardiac amyloid burden. In ^{99m}Tc-PYP imaging, whole-body imaging performed concurrently with chest imaging might allow evaluation of multi-organ systemic amyloid involvement and a substantial additional benefit of radionuclide evaluation of cardiac amyloidosis.

ACKNOWLEDGMENT The authors thank Editage for English language editing.

FUNDING SUPPORT AND AUTHOR DISCLOSURES

The authors have reported that they have no relationships relevant to the contents of this paper to disclose.

ADDRESS FOR CORRESPONDENCE: Dr Koji Takahashi, Department of Cardiology, Yawatahama City General Hospital, 1-638, Ohira, Yawatahama, Ehime 796-8502, Japan. E-mail: michitokitatsumasa@gmail.com.

REFERENCES

1. Singh V, Falk R, Di Carli MF, Kijewski M, Rapezzi C, Dorbala S. State-of-the-art radionuclide imaging in cardiac transthyretin amyloidosis. J Nucl Cardiol 2019;26:158–73.

2. Dorbala S, Ando Y, Bokhari S, et al. ASNC/AHA/ASE/EANM/HFSA/ISA/SCMR/SNMMI expert consensus recommendations for multimodality imaging in cardiac amyloidosis: part 1 of 2—evidence base and standardized methods of imaging. J Nucl Cardiol 2019;26:2065–123.

3. Sperry BW, Gonzalez MH, Brunken R, Cerqueira MD, Hanna M, Jaber WA. Non-cardiac uptake of technetium-99m pyrophosphate in transthyretin cardiac amyloidosis. J Nucl Cardiol 2019;26:1630–7.

4. Quarta CC, Gonzalez-Lopez E, Gilbertson JA, et al. Diagnostic sensitivity of abdominal fat aspiration in cardiac amyloidosis. Eur Heart J 2017;38:1905–8.

KEY WORDS abdominal fat, amyloidosis, bone-avid radiotracer, heart failure, transthyretin